The Berill Fault - first evidence of neotectonic faulting in southern Norway

Einar Anda, Lars Harald Blikra & Alvar Braathen

The Berill Fault of northern West Norway, documented here for the first time, is a N-S striking and moderately west dipping reverse fault with a throw of 2 to 4 metres. It is responsible for an escarpment, up to 6 metres in height, which can be followed across a prominent mountain ridge. The mapped escarpment, well displayed both in Quarternary sediments and bedrock, is approximately 2.5 km long. The bedrock of the hanging wall displays a number of clefts and fractures, as do overlying till and colluvium. In one part of the hanging wall, a 400 to 700 m large collapse field (slide block), has loosened and slid several tens of metres down slope. Since the fault affects Quaternary deposits of Younger Dryas age, movement must post-date the latter. Little modification of the faulted colluvial fans suggests that movement took place in the second half of the Holocene.

In a regional perspective, the fault may be associated with a series of strike parallel lineaments in the bedrock. If these lineaments constitute segments of a neotectonic fault zone, the throw versus surface-rupture-length ratio becomes approximately 2×10^{-4}, a realistic number compared to the high value of c. $1,2 \times 10^{-3}$ for the Berill Fault escarpment; the former number is more feasible when weighted against observations in other neotectonic regions. There is a higher frequency of rock avalanches near the Berill Fault and in the surrounding region, suggesting a link between rock-slope failures and a major palaeoseismic event.

Einar Anda, The County Council of Møre & Romsdal, N-6404 Molde, Norway. E-mail: Einar.Anda@mr-fylke.org
Lars Harald Blikra & Alvar Braathen, Geological Survey of Norway, N-7491 Trondheim.

Introduction

Neotectonism in northern Fennoscandia is documented by several postglacial faults, where of two are located in North Norway. They are likely associated with major earthquakes strong enough to produce significant deformation of the land surface (e.g., Kujansuu 1964; Lundquist & Lagerbäck 1976; Olesen 1988). In the course of the project 'Neotectonics in Norway' (Olesen et al. 2000; Dehls et al. 2000a,b), many neotectonic claims in South Norway were field checked; all were ultimately classified as being related to gravitational or erosional processes alone (Olesen et al. 2000), and hence could not be explained by remote tectonic forces. In this paper, we present the first neotectonic structure in southern Norway, the Berill Fault (Figs. 1 & 2). This structure is so-named because of its proximity to Berill in Møre, Norway. Significantly, it is situated in a region with numerous rock-avalanches, thus providing a link between bedrock failures and neotectonism. The presented dataset is limited, since detailed work on the Berill Fault is in progress. Our aim here is to describe the overall characteristics of the structure and briefly discuss implications of the fault throw/length ratio for palaeoseismisity and the distribution of rock-slope failures.

The most conspicuous neotectonic structure of Norway is the Stuorragurra Fault in Finnmark, which is a branch of the anastamosing Mierujavre-Sværholt Fault Zone (Olesen 1988; Olesen et al. 1992; Bungum & Lindholm 1997; Roberts et al. 1997; Dehls et al. 2000b). The Stuorragurra Fault dips to the southeast, and shows reverse displacement with a vertical throw in the range of 7 to 7.5 metres (Olesen et al. 2000). An earthquake of magnitude 4 in January 1996 (Bungum & Lindholm 1997) suggests that the structure is still seismically active (Dehls & Olesen 1999). A comparable structure is the Pärve Fault, one of several such structures in northern Sweden and Finland (Kujansuu 1964; Lundquist & Lagerbäck 1976; Lagerbäck 1979, 1990, 1992; Talbot & Slunga 1989). All these faults are thrusts, reactivating earlier formed structures in the basement. The reactivation is believed to be due to Mid Tertiary - Recent stresses caused by ridge-push (e.g., Lindholm et al. 2000). This force has a NW-SE orientation in northern Scandinavia (Spann et al. 1991; Fejerskov et al. 2000; Lindholm et al. 2000). In contrast, the neotectonic Nordmannsvik fault in Troms is a normal fault. It strikes NW-SE and dips moderately to the NE, with a vertical separation of 2-3 metres. It parallels the present maximum horizontal stress field (σ_H), which indicates a tensile type of faulting, consistent with the observed normal offset (Dehls et al. 2000b).
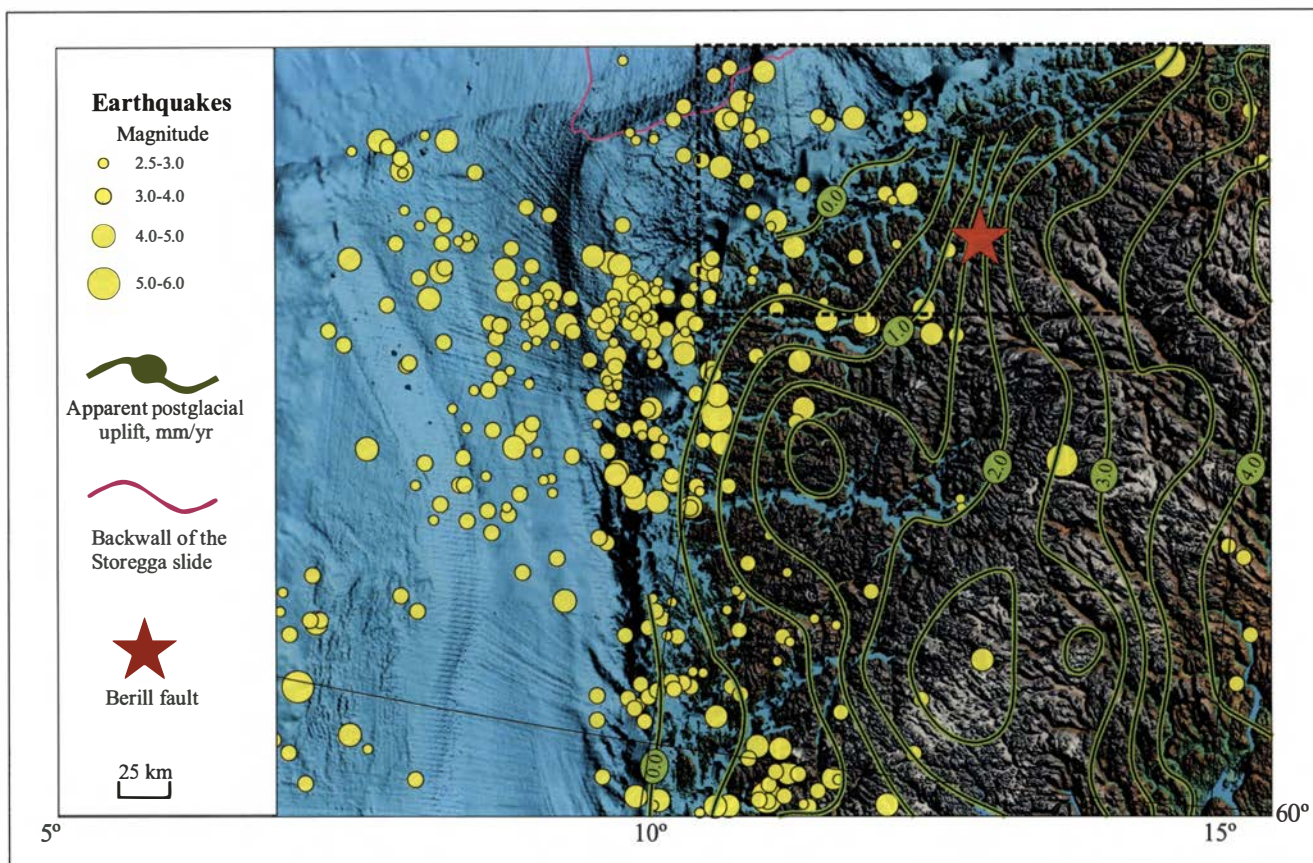
Fig. 1. Earthquake data (from Dehls et al. 2000a) and apparent land uplift plotted on a digital topography/bathymetry image base (modified from Dehls et al., 2000a). The location of the Berill Fault and the position of the map in figure 6 (box) are shown.

Ongoing evaluation of hazards related to potential rock avalanches in the Møre & Romsdal County (Blikra & Anda 1997, 1998; Blikra et al. 1999) can partly be approached through mapping of older avalanche events. Such events are located in specific regions. There are two main reasons for this: either steep and rugged topography, and/or earthquakes (Anda et. al, 2000; Blikra et al. 2001, 2002). The importance of earthquakes is discussed in an evaluation of historical, major earthquakes worldwide, many of which have caused major debris flows and rock failures (e.g., Keefer 1984; Jibson 1996). Strikingly, the Berill Fault is located in a region characterised by numerous rock avalanches, which raises a critical question: do pre-historical rock avalanches record major earthquakes of the past?

Regional setting

The Berill Fault is situated in the northern part of West Norway (Fig. 1), which presently has an E-W to NW-SE oriented compressional stress (σ_H) field in the upper part of the crust (e.g., Fejerskov et al. 2000; Lindholm et al. 2000). According to Anda (1986, 1995), steps in the regional topography indicate regional faulting in the Cainozoic and/or Mesozoic. Olesen et al. (2000)

argue that a Mesozoic timing is more realistic, seen in the light of the development of the regionally important, post-Caledonian Møre-Trøndelag Fault Complex. They state that the Tertiary exhumation has exposed a pre-existing basement topography that is visible today as wide fjords and mountain ridges. In a more recent context, Cainozoic uplift of Fennoscandia due to unloading following the latest glaciation has resulted in crustal doming. The deglaciation likely had two effects on the crust: It resulted in a sudden release of locked-in stress (Johnston 1987), and the gradual flexuring of the crust created stress that could have been strong enough to generate faulting (e.g., Gudmundsson 1999). With this in mind, one can conclude that the driving force for the Berill Fault probably was stresses of different origin. However, the most important force, seen in light of the N-S strike and reverse separation of the Berill Fault, is most likely ridge push.

The Berill Fault is situated in an area where the bedrock consists of various deep-crustal, quartzo-feldspathic migmatitic gneisses. These are intercalated with supracrustal rocks and enclose numerous lenses of meta-anorthosite, meta-gabbro/amphibolite, ultramafic rocks and, in the west, subordinate bodies of eclogite (e.g., Robinson 1995, Tveten et al. 1998). The ages of the rocks vary, but are mainly from the Mesoprotero-

zoic (e.g., Kullerud et al. 1986; Skår 1998). In the area around the Berill Fault, main lithologies are quartz-dioritic to granitic gneiss with some mica-rich layers (Tveten et al. 1998).

The Berill Fault

The Berill Fault (Figs. 2 and 3) was first identified on aerial photographs and, in year 2000, was confirmed during helicopter reconnaissance searching for rock-avalanche zones. Later field checking established its crosscutting relationship to Quaternary deposits.

The trace of the fault as mapped on the surface is approximately 2.5 km long, and the main structure reveals reverse displacement in the range of 2 to 4 m. It strikes N-S to NNW-SSE and dips moderately ($\approx$ 45°) west. A prominent 4-6 metres high escarpment can be traced from about 400 m above-sea-level (asl), near the valley floor, up the steep mountainside. It crosses the mountain ridge at 1200 m asl (Fig. 2), and continues down the north cliff-face before disappearing below talus. In the southern mountain slope the fault line is relatively straight, but makes a small lateral side step at 700 m asl.

In the south, the structure cuts through glacial till in the lowermost part before disappearing beneath collapsed slide blocks and fluvial and lake sediments on the valley floor. Upslope it truncates avalanche-dominated colluvial fans, as shown by its relationship to these geomorphic features (Figs. 2, 3 and 4). The glacial till, and especially the colluvial fan situated at 700 m asl, is offset for several meters along the fault (Figs. 4A and B). The bulk of the colluvial fan probably formed during the Younger Dryas period and possibly during later stages of the Holocene. There is no clear evidence that snow avalanches have modified the fault scarp significantly after faulting took place.

The fault scarp is well exposed in bedrock high on the mountain slope, where it can be traced for more than 1 km. The fault is mostly foliation-parallel, and consists of a single, distinct fracture near the ridge. This fracture branches into a 2-3 m wide fracture zone down-slope to the south, whereas in the northern cliff-face the fault consists of a 0.5-1 m thick breccia zone (Fig. 5C). The neotectonic fault likely reactivates an older structure, since in places it can be seen to follow 10-50 cm bands of cohesive cataclasite, commonly hosting epidote and quartz. Such fault rocks are diagnostic for faulting occurring at depths of several km.

The rocks in the hanging wall of the Berill Fault, i.e. the southern mountain slope west of the fault, show significant surface deformation, whereas the footwall section is undisturbed. This deformation is revealed as collapse of the mountainside below an upper-bounding fracture surface (Figs. 2 and 3), in what can be classifed
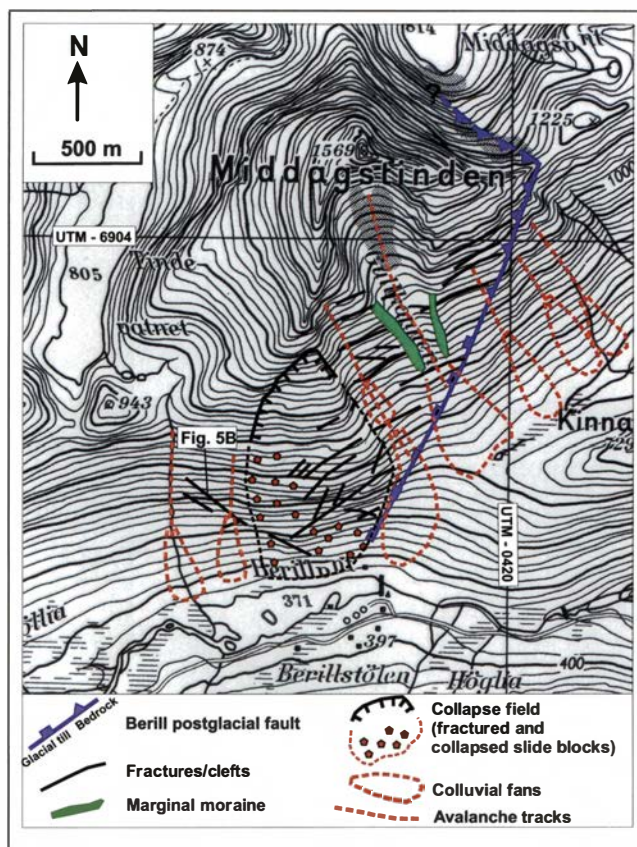

Fig. 2. Map showing the Berill Fault, hangingwall fractures and clefts, and the major Quaternary geomorphic elements. The fault shows reverse separation, strikes approximately N-S and dips moderately W (45°).

Fig. 3. Aerial photograph of the Berill Fault, truncating glacial till and colluvial fans.
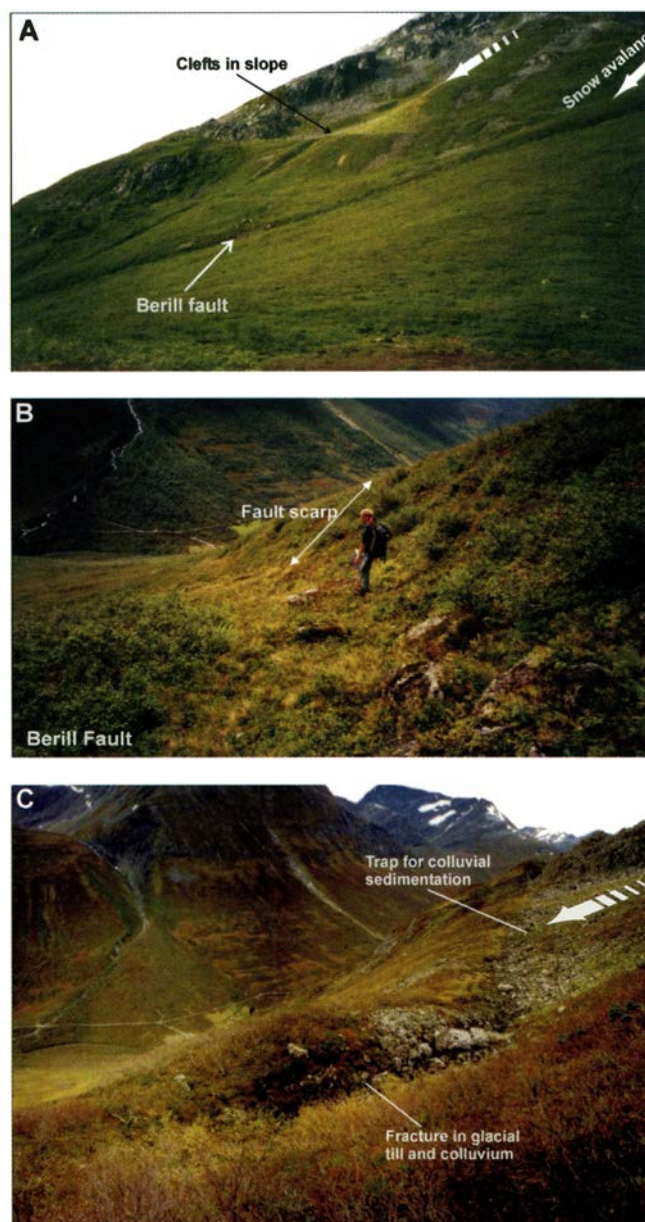
Fig. 4. Details of the Berill Fault. A: Overview photograph of the Berill Fault, seen from the southeast. Note that the fault clearly truncates the colluvial fan (up to the right). B: The fault cuts into the colluvial fans in the middle part of the photograph. The fault scarp is not showing indications of later modification by creep or avalanche processes. The view towards north. C: Fracture cutting into glacial debris and colluvial fans to the west of the Berill Fault. The cleft terminates at the Berill Fault. Note that recent snow-avalanche dominated fans fill the depression at the right-hand side. View towards NNE.

as a "collapse field" (Braathen & Blikra, unpublished data). The 400x600m large collapsed field, west of the Berill Fault, is characterized by deep clefts and a rough surface of rotated blocks. Open fractures (crevasses) bound the blocks upslope together with cross-fractures, which define the individual block margins (Fig. 2 and 3). A series of crevasses and large fractures characterise the rock and glacial-till surface outside the collapse field, some of them acting as traps for debris transpor-

ted by snow avalanches (Figs. 4C and 5B). The fractures are 300-600 m long, and all terminate along the fault zone (Figs. 2 and 3). Except for a few structures in the southernmost part, all strike SW-NE, i.e. nearly parallel to the topographic slope. Hence, they have an oblique orientation to the Berill Fault.

The Berill Fault belongs to the Mandal-Molde lineament zone (Gabrielsen et al. 2002), which is characterized by predominantly N-S lineaments. Reconnaissance of the region has revealed other N-S lineaments that may relate to the Berill Fault. They have steep orientations, and appear strikingly "fresh" without significant sediment filling or clear signs of glacial-related erosion. Unfortunately, the age of movement on these lineaments cannot be constrained, since temporal markers, such as Holocene sediments, have yet to be found. The best example is located approximately 10 km south of the Berill Fault, where a 5-m wide and roughly 10-km long fracture zone is seen as a surface scar in fresh bedrock. Within the zone, there are layers and lenses of fault rocks (cataclasite) associated with epidote and quartz veins, strikingly similar to the old fault rocks found along the Berill Fault. One can speculate that the Berill Fault is the most prominent structure within a N-S striking, neotectonic fault zone. This would make the neotectonic structure much longer that the 2.5-km surface rupture observed along the Berill Fault (see Discussion).

Timing of faulting

The Berill Fault is probably formed during the second half of the Holocene. This is so because well-defined colluvial fans of the Younger Dryas period (13.000-11.500 cal. years BP) are clearly truncated by the fault. Blikra & Nemec (1998) conclude that a high frequency of snow avalanches, with related colluvium, characterise the Younger Dryas period, and also periods during the second half of the Holocene. Since the fault scarp is slightly modified by the erosion and deposition of colluvium, the overall observations are most consistent with faulting during the second half of the Holocene.

From the study of rock avalanches in Møre & Romsdal, it is clear that they occur in distinct regions (Fig. 6). Studies of historical earthquakes worldwide have shown that many of these trigger different types of rock failure (e.g. Keefer 1984; Jibson 1996). The spatial occurrence of individual events, especially if dated, may therefore shed light on palaeoseismic activity. The review by Jibson (1996) also indicates that large rock avalanches are the type of avalanche or slide activity with the greatest potential in such studies. The Berill Fault occurs in a region characterized by a high frequency of rock-avalanches (Fig. 6). The southern part of the mountain slope west of the Berill Fault shows evidence of extensive gravitational sliding, and at least
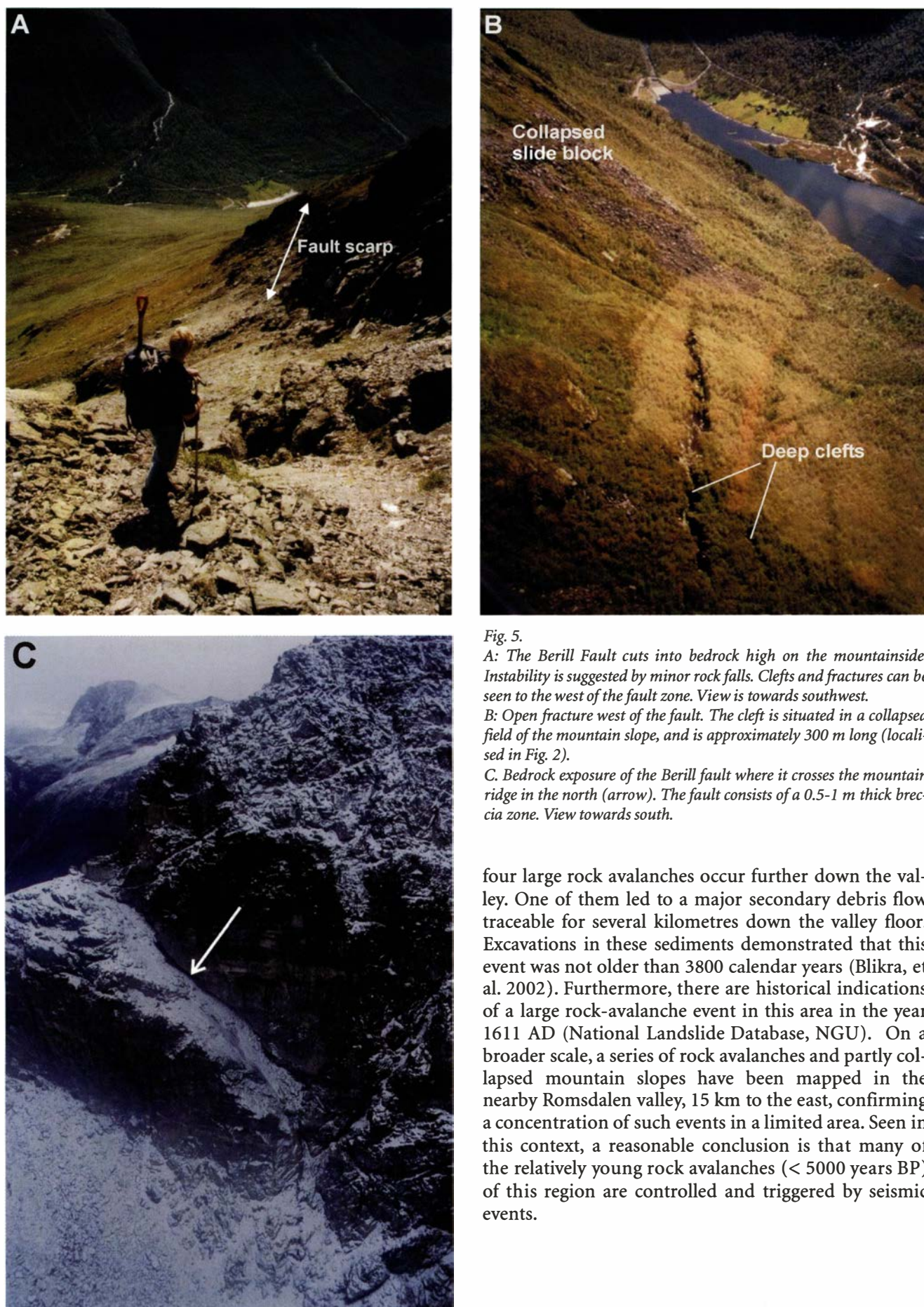
Fig. 5.
A: The Berill Fault cuts into bedrock high on the mountainside. Instability is suggested by minor rock falls. Clefts and fractures can be seen to the west of the fault zone. View is towards southwest.
B: Open fracture west of the fault. The cleft is situated in a collapsed field of the mountain slope, and is approximately 300 m long (localised in Fig. 2).
C. Bedrock exposure of the Berill fault where it crosses the mountain ridge in the north (arrow). The fault consists of a 0.5-1 m thick breccia zone. View towards south.

four large rock avalanches occur further down the valley. One of them led to a major secondary debris flow traceable for several kilometres down the valley floor. Excavations in these sediments demonstrated that this event was not older than 3800 calendar years (Blikra, et al. 2002). Furthermore, there are historical indications of a large rock-avalanche event in this area in the year 1611 AD (National Landslide Database, NGU). On a broader scale, a series of rock avalanches and partly collapsed mountain slopes have been mapped in the nearby Romsdalen valley, 15 km to the east, confirming a concentration of such events in a limited area. Seen in this context, a reasonable conclusion is that many of the relatively young rock avalanches (< 5000 years BP) of this region are controlled and triggered by seismic events.
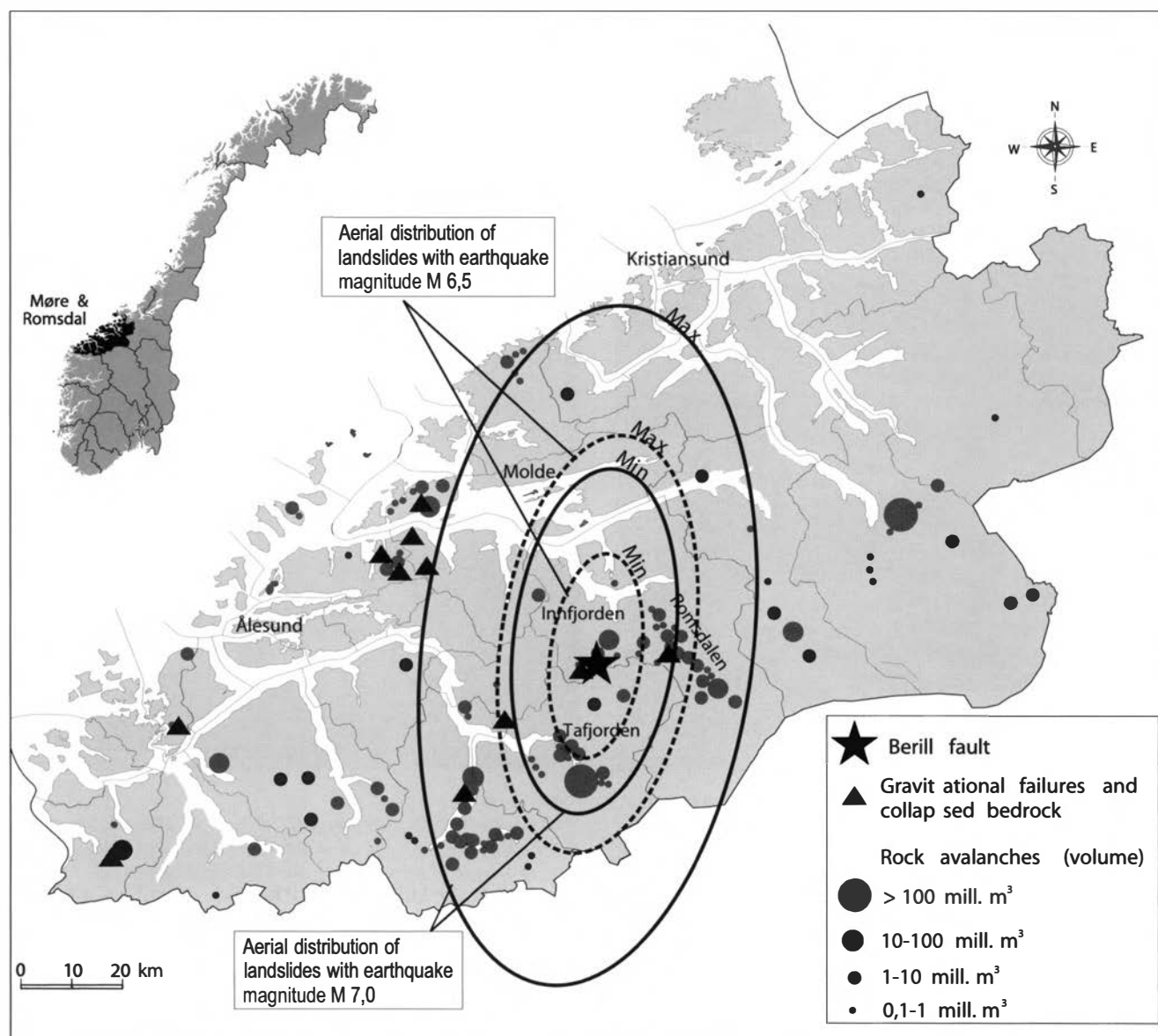
Fig. 6. Map of Møre & Romsdal County, showing the regional distribution of large rock avalanches and areas were mountainsides show sign of collapse (gravitational instabilities), as well as the location of the Berill Fault. Aerial distribution of potential landslides during earthquake events of magnitude 6.5 and 7.0 is indicated in the Innfjorden – Romsdalen area (the Berill Fault is located near the centre of the area). Potential areas affected by landslides are derived from the relationship found by Keefer (1984).

Discussion

The Berill Fault is a neotectonic structure because it truncates Younger Dryas sediments. It has a semi-linear trend and crosses a mountain slope and ridge. Characteristically, the hanging wall is highly fractured, consistent with increased strain above the fault, and probably related to accommodation of the hanging wall during fault-slip event(s).

Reverse fault throw in the range of 2-4 m is consistent with a major seismic event, possibly in the range of magnitude 6.5 to 7.5 (Carver & McCalpin 1996), i.e. somewhat smaller than that indicated for the Stuora-gurra Fault of Finnmark (Dehls & Olesen 1999; 7 m throw versus 80 km length gives a ratio ~ 1 x 10^-4). However, when discussing the earthquake magnitude,

one has to bear in mind that the calculated throw-length ratio of approximately $1,2 \times 10^{-3}$ for the Berill Fault (2-4 m throw and 2.5 km length) is high when compared to other surface-rupturing faults in a global perspective (Wells & Coppersmith 1994), where most faults have a throw/length ratio of 1×10^{-4}. In this context, a continuation of the Berill Fault by a soft-link step-over to N-S lineaments observed farther south, would give a rupture length in the range of 15 km. If valid, this throw/length ratio (3-m/15-km) would be in the order of 2×10^{-4}, more consistent with global data. This surface rupture ratio indicates an earthquake slightly above magnitude 6.0 on the Richter scale. Alternatively, the offset could relate to multiple, smaller events along the Berill Fault, albeit data from other tectonically active regions suggest that most observed sur-

face-rupturing faults are caused by a single event. This is so basically because the erosional denudation of the fault escarpment outpaces the reoccurrence of a large earthquake (Carven & McCalpin 1996). Planned excavation of the fault in the valley fill may confirm the temporal development, as well as the exact time of faulting. The spatial occurrence of debris and rock failures and their age relationship can be used for palaeoseismic analysis (Keefer 1984; Jibson 1996). Review of historical and recent data on seismically induced landslides shows that the full range of landslide types can be initiated by seismic activity, and 81% of all slope failures occur in regions with mean horizontal peak ground acceleration (PGA) greater than 1.5 m/s^2 (Sitar & Kahazai 2001). A PGA equal to or larger than 1.5 m/s^2 is comparable to an earthquake above magnitude 6 within a distance of 20-30 km. The relationship between earthquake magnitude and area affected by landslides has been analysed by Keefer (1984), who concludes that earthquakes of magnitude 6.5 will affect an area of 800-4000 km^2, and earthquakes of magnitude 7.0 an area of 3000-12000 km^2. Commonly, the area affected by collapse and slides has an elliptical shape (Adams 1981).

In Møre, the main areas of rock avalanches and gravitational bedrock failures are located near the Berill Fault, as shown in Figure 6. Concentrations are found around Innfjorden, the Romsdalen valley and Tafjorden. For both of these areas, the total spatial extent of sites with rock avalanches and gravitational bedrock failures is c. 30 km in an east-west direction and c. 40 km in a north-south direction, giving an area of c. 1000 km^2. Areas of this size are consistent with an earthquake of magnitude 6.3-6.7. In a coastal area west of Molde, the limiting spatial extent of a cluster of rock-slope failures is about 25 km long and 15 km wide, giving an area of about 300-350 km^2 (Fig. 6), which would then imply an earthquake of magnitude 5.5-6.2. However, according to Keefer (1984), deep bedrock failures require an earthquake greater than magnitude 6.5, hence larger than that predicted from the spatial ellipse. Besides, a smaller earthquake would promote other types of mass failure, which would then be expected to dominate the area. The predicted earthquake magnitudes based on the distribution of rock avalanches is thus probably too low. If an earthquake related to the Berill Fault controlled the distribution of the rock avalanches in this region, and taking into consideration the length (10-15 km?) and fault throw (2-4-m), a conservative estimate of this earthquake is between magnitudes 6 and 6.5. The area that would be affected by landslides and avalanches during an earthquake event of either magnitude 6.5 or 7 is indicated in Figure 6.

The Berill Fault is younger than the Younger Dryas period (13.000-11.500 years before the present), and the minor modification of the fault scarp suggests that the faulting occurred during the second half of the Holocene. If this is correct, then postglacial faulting in this region is unrelated to the time shortly after deglaciation, which is the period with highest post-glacial, isostatic uplift. Albeit the rate of uplift at the time of faulting is unknown, it is worth mentioning that this area is situated in a zone with one of the highest gradients of present land uplift in western Norway (Fig. 1; Dehls et al. 2000a); and hence has a potential for surface deformation. However, when the N-S orientation and reverse separation of the fault is considered, the most important driving force for faulting is likely related to the mid-oceanic ridge push.

Conclusions and future work

The Berill Fault is a neotectonic structure formed after the Yonger Dryas period, probably during the second half of the Holocene. It strikes N-S, dips moderately west, and shows reverse separation in the range of 2-4 m. The mapped fault escarpment is approximately 2.5-km long. On the more speculative side, the Berill Fault may be a segment of a regional N-S fault zone consisting of a series of lineaments which together may have experienced neotectonic activity.

Several topics are critical for further understanding of the importance of the Berill Fault. Firstly, more precise age determination of the faulting event can be approached through excavation of the fault scarp in Younger Dryas sediments. This may also shed light on the case for one or several faulting events. Secondly, detailed studies of the fault in bedrock may confirm whether the fault is truly reverse or has an oblique component. This has implications for the assessment of the magnitude of an earthquake, as well as for the interpretation of the driving force for faulting. Thirdly, new good localities along other lineaments of the N-S lineament zone may justify or exclude a link between the Berill Fault and other, nearby structures. Finally, on a regional scale, more precise age determinations of rock-slope failures, and especially if they can be temporally correlated, would clarify a possible link between rock avalanches and earthquakes of the past.

References

Adams, J. 1981: Earthquake-dammed lakes in New Zealand. *Geology 9*, 215-219.

Anda, E. 1986: Nordvestlandet: Regional topografi og den tertiære landhevingen. Abstract. *Geolognytt 21*, p. 5.

Anda, E. 1995: Romsdalen og Romsdalsfjorden. Hovedtrekkene i landskapet. p 14-34. In: Sanden, J.: *Romsdalen natur og kultur.* Romsdalsmuseet årbok, 186 pp.

Anda, E. & Blikra, L.H. 1998: Rock-avalanche hazard in Møre & Romsdal, western Norway. *Norwegian Geotechnical Institute Publication 203*, 53-57.

Anda, E., Blikra, L.H. & Longva, O. 2000: Large-scale slope failures in Møre and Romsdal - Palaeoseismic evidence? *In* Dehls, J. & Olesen, O. (eds.) *Neotectonics in Norway,* Annual Technical Report. *Norges geologiske undersøkelse Report 2000.01*, 20-25.

Blikra, L.H. & Anda, E. 1997: Large rock avalanches in Møre og Romsdal, western Norway. *Norges geologiske undersøkelse Bulletin 433*, 44-45.

Blikra, L.H., Anda, E., Braathen, A., Stalsberg, K. & Longva, O. 2002: Rock avalanches, gravitational bedrock fractures and neotectonic faults onshore western Norway: Examples, regional distribution and triggering mechanisms. *Norges geologiske undersøkelse Report 2002.016*, 48 pp.

Blikra, L.H., Anda, E. & Longva, O. 1999: Fjellskredprosjektet i Møre og Romsdal: Status og planer. *Norges geologiske undersøkelse Report 99.120*, 21 pp.

Blikra, L.H., Braathen, A. & Skurtveit, E. 2001: Hazard evaluation of rock avalanches; the Baraldsnes area. *Norges geologiske undersøkelse Report 2001.108*, 48 pp.

Blikra, L.H. & Nemec, W. 1998: Postglacial colluvium in western Norway: depositional processes, facies and palaeoclimatic record. *Sedimentology 45*, 909-959.

Bungum, H. & Lindholm, C. 1997. Seismo- and neotectonics in Finnmark, Kola Peninsula and the southern Barents Sea. Part 2: Seismological analysis and seismotectonics. *Tectonophysics 270*, 15-28.

Carver, G.A. & McCalpin, J.P. 1994: Palaeoseismology of compressional tectonic environments. *In* McCalpin, J.P. (ed.) *Paleoseismology.* International Geophysics Series 62, 183-270. Academic press.

Dehls, J. & Olesen, O. 1999: Neotectonics in Norway. Annual technical report. *Norges geologiske undersøkelse Report 99.007*, 206 pp.

Dehls, J., Olesen, O., Bungum, H., Hicks, E.C., Lindholm, C.D. & Riis, F. 2000a: Neotectonic map: Norway and adjacent areas. *Norges geologiske undersøkelse.*

Dehls, J.F., Olesen, O., Olsen, L. & Blikra, L.H. 2000b: Neotectonic faulting in northern Norway; the Stuoragurra and Nordmannvikdalen faults. *Quaternary Science Reviews 19*, 1447-1460.

Fejerskov, M., Lindholm, C., Larsen, B.T. & Nøttvedt, A. 2000: *Stress map, North Atlantic area, scale 1:3 million.* Integrated basin studies, Dynamics of the Norwegian Continental margin.

Gabrielsen, R.H., Braathen, A., Dehls, J. & Roberts, D. 2002: Tectonic lineaments of Norway. *Norwegian Journal of Geology (NGT) 82*, 153-174.

Gudmundsson, A. 1999. Postglacial crustal doming, stresses and fracture formation with application to Norway. *Tectonophysics 307*, 407-419.

Jibson, R.W. 1994: Using landslides for Palaeoseismic analysis. *In*: McCalpin (ed.) *Paleoseismology.* International Geophysics Series 62, 397-438. Academic Press.

Johnston, A.C. 1987: Suppression of earthquakes by large continental ice sheets. *Nature 330*, 467-469.

Keefer, D.K. 1984: Landslides caused by earthquakes. *Geological Society of America Bulletin 95*, 406-421.

Kujansuu, R. 1964: Nuorista sirroksista Lapissa. Summary: recent faults in Lapland. *Geologi 16*, 30-36.

Kullerud, L., Tørudbakken, B. & Ilebekk, S. 1986: A compilation of radiometric age determinations from the Western Gneiss Region, South Norway. *Norges geologiske undersøkelse Bulletin 406*, 17-42.

Lagerbäck, R. 1979: Neotectonic structures in northern Sweden. *Geologiska Föreningens i Stockholm Förhandlingar 100*, 271-278.

Lagerbäck, R. 1990: Late Quaternary faulting and paleoseismicity in northern Fennoscandia with particular reference to the Lansjärv area, northern Sweden. *Geologiska Föreningens i Stockholm Förhandlingar 112*, 333-354.

Lagerbäck, R. 1992: Dating of late Quternary faulting in northern Sweden. *Journal of the Geological Society of London 149*, 285-291.

Lindholm, C.D., Bungum, H., Hicks, E. & Villagran, A. 2000: Crustal stress and tectonics in Norwegian regions determined from earthquake focal mechanisms. *Geological Society of London Special Publication 167*, 429-440.

Lundquist, J. & Lagerbäck, R. 1976: The Pärve Fault: A late-glacial fault in the Precambrian of Swedish Lapland. *Geologiska Föreningens i Stockholm Förhandlingar 98*, 45-51.

Olesen, O., Henkel, H., Lile, O.B., Mauring, E. & Rønning, J.S. 1992: Geophysical investigations of the Stuoragurra postglacial Fault, Finnmark, northern Norway. *Journal of Pure and Applied Geophysics 29*, 95-118.

Olesen, O. 1988: The Stuoragurra Fault, evidence of neotectonics in the Precambrian of Finnmark, northern Norway. *Norges Geologiske Tidsskrift 68*, 107-118.

Olesen, O., et al. 2000: Neotectonics in Norway, Final report. *Norges geologiske undersøkelse Report 2000.002*, 120 pp.

Roberts, D., Olesen, O. & Karpuz, M.R. 1997: Seismo- and neotectonics in Finnmark, Kola Peninsula and the southern Barents Sea. Part 1: Geological and neotectonic framework. *Tectonophysics 270*, 1-13.

Robinson, P., 1995. Extension of Trollheimen tectono-stratigraphic sequence in deep synclines near Molde and Brattvåg, Western Gneiss Region, southern Norway. *Norsk Geologisk Tidsskrift 75*, 181-198.

Sitar, N. & Khazai, B. 2001: Characteristics of seismically induced landslides in recent earthquakes. *In* Kühne, M. Einstein, H.H., Krauter, E., Klapperich, H. & Pöttler, R. (eds.) *International Conference on Landslides, Causes, Impacts and Countermeasures VGE.* Davos, Switzerland.

Skår, Ø. 1998: The Proterozoic and Early Paleozoic evolution of the southern parts of the Western Gneiss Complex, Norway. Dr. Sci. thesis, University of Bergen.

Spann, H., Brudy, M. & Fuchs, K. 1991: Stress evaluation in offshore regions of Norway. *Terra Nova 3*, 148-152.

Talbot, C.J. & Slunga, R. 1989: Patterns of active shear in Scandinavia. *In* Gregersen, S. & Basham, P.W. (eds.) *Earthquakes at the North-Atlantic passive margins: Neotectonics and postglacial rebound,* 441-466. Kluwer Press.

Tveten, E., Lutro, O. & Thorsnes, T. 1998: *Berggrunnskart Ålesund, M 1:250,000.* Norges geologiske undersøkelse.

Wells, D. L. & Coppersmith, K. J. 1994: Empirical relationships among magnitude, rupture length, rupture area, and surface displacement. *Bulletin of the Seismological Society of America 84*, 974-1002.